Theor. Appl. Climatol. (2009) 95: 111–123
DOI 10.1007/s00704-007-0362-9
Printed in The Netherlands

Theoretical and Applied Climatology

[1] Department of Climatology and Landscape Ecology, University of Szeged, Szeged, Hungary
[2] Urban Climate Group, Physical Geography, Göteborg University, Göteborg, Sweden

Computing continuous sky view factors using 3D urban raster and vector databases: comparison and application to urban climate

T. Gál[1], F. Lindberg[2], J. Unger[1]

With 13 Figures

Received 28 December 2006; Accepted 17 September 2007; Published online 8 January 2008

Summary

The use of high resolution 3D urban raster and vector databases in urban climatology is presented. It applies two different methods to the calculation of continuous sky view factors (SVF), compares their values and considers their usefulness and limitations in urban climate studies. It shows and evaluates the relationship between urban geometry, quantified by SVF, and intra-urban nocturnal temperature variations using areal means in the whole urban area of Szeged, a city located in southeast Hungary. Results from the vector and raster models shows similar SVF values ($r^2 = 0.9827$). The usefulness of using areal means in SVF-temperature relations is confirmed. The vector and the raster approaches to the derivation of areal means of SVF are both shown to be powerful tools to obtain a general picture of the geometrical conditions of an urban environment.

1. Introduction

Urban areas exhibit striking and continuing man-made changes in land-use, especially surface properties such as their materials and geometric form. As a consequence, urban environments modify the surface energy and water balance which often results in higher nocturnal urban temperatures compared to their more natural surroundings (urban heat island – UHI, ΔT). Different heat islands can be distinguished: beneath the surface, at the surface, in the urban canopy layer (UCL) and the urban boundary layer (Oke 1982). As in the case here, the UHI is typically presented as a temperature difference between the air within the UCL (extends from the ground up to about mean roof level) and that measured in a rural area outside the settlement at similar heights. Generally, its strongest development occurs at night when the heat, stored in the daytime, is released more slowly than the rural area and therefore does not cool off as fast (Landsberg 1981; Oke 1987).

Nocturnal cooling processes are primarily forced by outgoing long wave radiation. In cities, narrow streets and high buildings create deep canyons. This 3D geometrical configuration plays an important role in regulating long-wave radiative heat loss. Due to the fact that only a smaller part of the sky is seen from the surface (because of the horizontal and vertical unevenness of the surface elements), the nocturnal long wave radiation loss is more restricted here than in rural areas.

Correspondence: Tamás Gál, Department of Climatology and Landscape Ecology, University of Szeged, PO Box 653, 6701 Szeged, Hungary, e-mail: tgal@geo.u-szeged.hu

Therefore, urban geometry is one important factor contributing to intra-urban temperature variations below roof level (e.g. Oke 1981; Eliasson 1996). The sky view factor (SVF) is often used to describe the urban geometry but also other measures are also used e.g. height-to-width ratio (Goh and Chang 1999) and frontal area index (Grimmond and Oke 1999). By definition, SVF is the ratio of the radiation received (or emitted) by a planar surface to the radiation emitted (or received) by the entire hemispheric environment (Watson and Johnson 1987). It is a dimensionless measure between zero and one, representing totally obstructed and free spaces, respectively (Oke 1988). It is expected that a region of a city with a smaller SVF should cool off more slowly since the sky is obstructed by buildings and the long-wave radiation tend to be trapped in the UCL.

Of course, other factors also contribute to the development of the UHI (built-up or paved area ratio, heat released by human activity, etc. see e.g. Oke (1987)). But the focus of this investigation is on urban surface geometry – UHI relationship using one of the most useful measure of surface geometry, the SVF as earlier studies have shown (e.g. Oke 1981; Svensson 2004).

Modern GIS-based 3D models of cities open new possibilities to describe and develop measures of geometry applicable in urban climate research (e.g. Ratti and Richens 1999). Ratti (2001) utilizes high resolution raster DEMs for computing images of continuous sky view factors. His SVF-model has been validated and has generated accurate results (Brown et al. 2001; Lindberg 2005).

A comprehensive literature review of SVF-temperature variations within urban areas by Unger (2004) showed that results from previous studies can be rather contradictory, especially if comparisons are based on a few element pairs measured at selected sites within the city. Unger (2004, 2007) suggests that further studies should focus on comparison between areal means of both geometry and temperature variations.

The overall purpose of the present study is to consider the application of high resolution 3D urban raster and vector databases in urban climatology. The specific objectives are (1) to present and apply two different methods to calculate SVFs, both based on urban 3D models; (2) to compare the two methods and consider their limitations and potentials in urban climate studies; (3) to study and evaluate the relationship between urban geometry as quantified by SVF and intra-urban nocturnal temperature variations using areal means for the whole urban area of Szeged, Hungary.

2. Study area and temperature measurements

Szeged (46° N, 20° E) is a city located in south-east Hungary, in the southern part of the Great Hungarian Plain at 79 m above sea level on a flat plain (Fig. 1). According to Trewartha's classification Szeged belongs to the climatic type D.1 (continental climate with longer warm season), similarly to the predominant part of the country (Unger 1996). While the administrative area of Szeged is 281 km^2, the urbanized area is only around 30 km^2. The avenue-boulevard structure

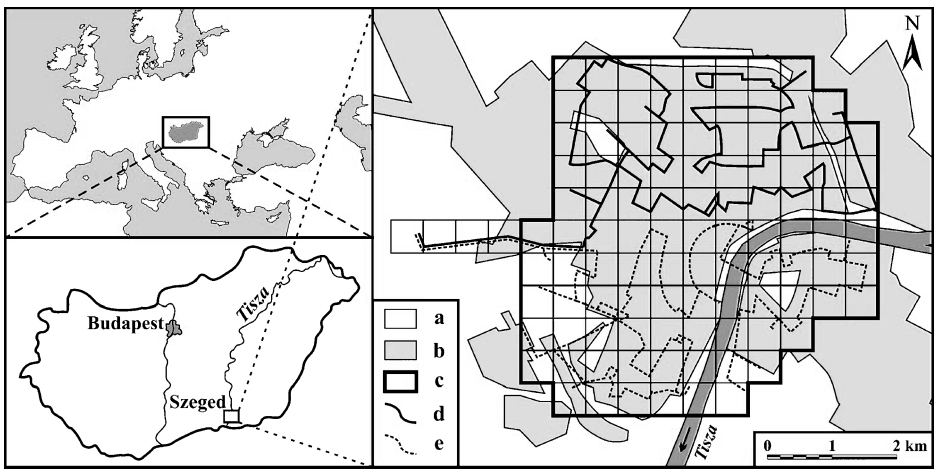

Fig. 1. Location of Szeged in Europe and in Hungary, as well as the grid network in Szeged: (a) open area, (b) built-up area, (c) border of the investigated area, (d, e) measurement routes

of the town was built to follow the axis of the river Tisza. There are no other water bodies in the vicinity of the city. The population was about 160,000 in the investigated years (2002–2003).

In order to determine the spatial variation of temperature in the city the study area was divided into two sectors and subdivided further into 500 m × 500 m cells (Fig. 1). It consists of 107 cells covering the urban and suburban parts of Szeged (26.75 km^2). The outlying parts of the city, characterized by villages and rural features, are not included in the grid, with the exception of four cells on the western side of the area. This latter part is necessary to determine urban-rural temperature contrasts and it is not included in the investigated area (103 cells).

According to Oke (2004) the circle of influence on a screen level (~1.5 m) temperature is thought to have a radius of about 0.5 km typically, but this is likely to depend upon the building density. So the 500 m mesh is reasonable to simulate night temperatures in urban canopies.

Mobile temperature measurements were made at night by two cars in two sectors at the same time during a one-year period (April 2002 – March 2003), altogether 35 times approximately with 10-day frequency (Unger 2006). In studying UHI, the quantity of interest is frequently not the absolute urban temperature, but the difference between the urban and rural areas. The possibility of errors due to inter-sensor differences is thereby removed (Streutker 2003).

On the basis of previous studies, data collection was carried out in such a way that observations took place around the expected time of maximum development of the UHI, about 4 h after sunset based on previous research (e.g. Oke 1981) and on earlier measurements in Szeged (e.g. Unger et al. 2001). After averaging the 15–20 measurement values in each grid cell, time adjustments were applied back to a reference time. The approach assumed an approximately linear change in air temperature with time (which was checked against continuous records at the automatic weather station at the University of Szeged).

Due to the size of the study area as well as the length of the measurement routes, the area was divided into 2 sectors. Routes were designed so that all cells were traversed at least once on the way out and back (Fig. 1). It took about 3 h to obtain measurements on the outward and inward traverse legs and were conducted in all weather conditions, except for rain. The cars reached the turning point at the reference time (4 h after sunset). The temperature observations were carried out by an automatic radiation-shielded sensor connected to a digital data logger that sampled every 10 s. In order to diminish the thermal disturbance due to the car, the sensor was attached to a bar extending 0.6 m ahead of the car at the height of 1.45 m above the ground. Due to the need for efficient ventilation and to obtain a high density of data, the speed of the car was 20 to 30 $km\,h^{-1}$ hence data were gathered from every 55 to 83 m travelled. Measurements were taken after the peak traffic hours had passed so stoppages due to red lights or other barriers were seldom: data taken when the car was stopped for the any reason was later deleted from the database. Height-dependent temperature corrections are not an issue because the area is essentially flat (<8 m elevation difference).

ΔT values were determined by referring cell averages (T_{cell}) to the temperature average of the westernmost cell ($T_{cell(W)}$) of the study area, located in countryside:

$$\Delta T = T_{cell} - T_{cell(W)}$$

The westernmost cell consists of agricultural land, mainly fields of non-irrigated wheat, sunflowers and maize, which are representative of the rural surroundings of Szeged (Fig. 1).

3. Methods: 3D building database, SVF calculations

The creation of the applied 3D building database for Szeged was based on local municipality data of building footprints and aerial photographs to determine individual building heights. To cross-check, theodolite measurements of heights were conducted giving the mean ratio of the differences compared to the database was about 5%. The database covers the whole study area and consists of more than 22,000 buildings. Small buildings are difficult to determine from the aerial photographs, and further their heat absorption and emission are negligible. Thus, buildings smaller than 15 m^2 were excluded from the database. The Digital Elevation Model (DEM) for Szeged represents a bare surface with a small vertical

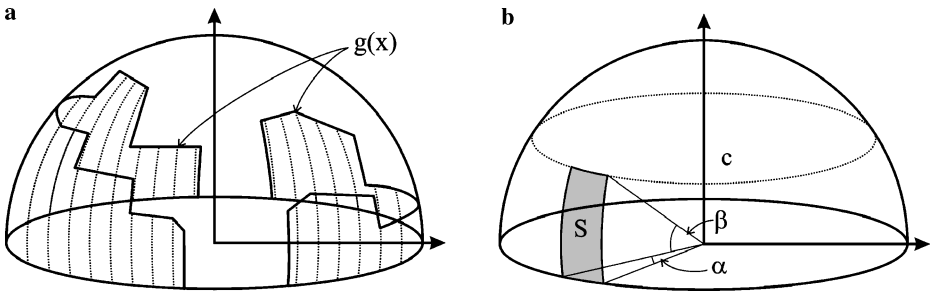

Fig. 2. (**a**) Polygon g(x) as the border of the visible sky and division of the overlying hemisphere under g(x) into equal slices by angle α (heights are equal to the g(x) values in the middle points of the intervals), (**b**) a slice of a 'width' of α (S) of a basin with an elevation angle β

variation of the surface (75.5–83 m a.s.l.). Both vector and raster data are in the Unified National Projection (EOV in Hungarian). The creation of the database is described in detail in Unger (2006, 2007).

Our assessment of the strength of the SVF-UHI relationship is almost the same if the SVF calculation is based at screen- or ground level (Unger 2007). Here, SVF calculations refer to points at ground level.

3.1 SVF calculation using an urban vector database

The 3D building database is a model of the real world. It represents a simplified view of the urban surface made up of flat-roofed buildings only. Further the walls of any given building have the same height.

The projection of every building on the sky is managed like the projection of their walls visible from a given surface point and polygon g(x) is the border of the visible sky (Fig. 2a). After dividing the hemisphere equally into slices by rotation angle α, 'rectangles' are drawn whose heights are equal to the g(x) values in the middle points of the intervals.

SVF values for a common geometric arrangements are given by Oke (1987). For the case of a regular basin, where β is the elevation angle from the centre to the wall, the SVF value is (referring to the basin centre): $\mathrm{SVF}_{\mathrm{basin}} = \cos^2\beta$. So the view factor (VF) of a basin with an elevation angle β is $\mathrm{VF}_{\mathrm{basin}} = 1 - \cos^2\beta = \sin^2\beta$, therefore the view factor for a slice (S) with a width of α (Fig. 2b) can be written as:

$$\mathrm{VF_S} = \sin^2\beta \cdot (\alpha/360)$$

The algorithm draws a line by the angle α from the selected point and along that line it searches a single building which obstructs the largest part from the sky at that direction. That is, which building has the largest elevation angle β within a certain distance at that direction. The accuracy of the algorithm depends on the magnitude of the rotation angle (α). Smaller α angles result in more accurate estimation of SVF (given here as $\mathrm{SVF_v}$ – i.e. SVF computed by vector based method) but require longer computation time. The length of the lines is set by the user. After calculating the VF values by slices they are added and the sum is subtracted from 1 to get the $\mathrm{SVF_v}$.

ESRI ArcView 3.2 software (www.esri.com) has a built-in object-oriented language (Avenue) appropriate for our purpose. The software is programmable so that every element is accessible (Souza et al. 2003). Our application is compiled from 9 scripts (graphical surface, control of the parameters, calculation of $\mathrm{SVF_v}$, etc.). Figure 3 schematically illustrates the developed algorithm. Values for two parameters have to be selected: (i) the radius of the area around the site where the algorithm takes into account the heights and positions of the building, and (ii) the interval of the rotation angle (α) which determines the density of the target lines starting from the site. In our case a radius of 200 m and a rotation angle of 1° seemed appropriate (details in Unger 2007).

The $\mathrm{SVF_v}$ was determined in a point network that covers the entire investigated area. The elevation of points was derived from a DEM covering the study area. To select optimal point resolution the precision of the database and the

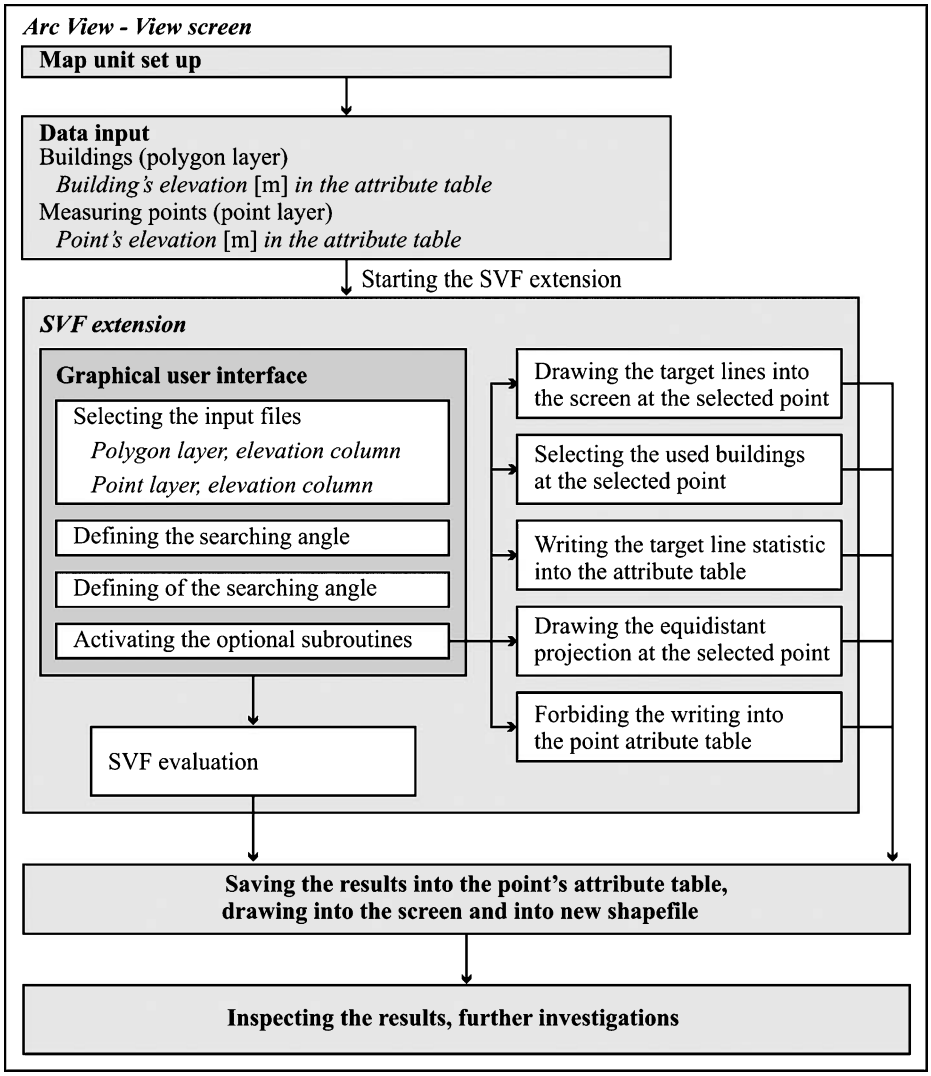

Fig. 3. Schematic description of the algorithm for the SVF calculation using a vector database

necessary computing time must be considered. We found a 5 m resolution is appropriate to obtain continuous spatial distribution of the SVF_v and to reveal the main characteristics of the distribution. Application of this resolution resulted in a total of 1,030,000 points in the 103 study cells.

After all individual values of SVF_v were derived, cell averages were computed. For this, points overlapped by the buildings were deleted from the point network so that the relationship between the SVF_v and the thermal characteristics of the urban canopy layer could be examined (Fig. 4). Thus, inclusion of SVF_v values of these points in the calculation of cell averages would be inappropriate. After the deletion, altogether 897,188 points were left in the investigated area. The number of point was different (ranging between 6171 and 9900) in cells depending on the total footprint area of the buildings. The SVF_v calculation was run for this point network on the ground surface. It needed one day to compute the SVF_v values for one cell. Therefore computation for the complete study area took several days, but not more than two weeks, if more than one computer was utilized. The outcome is a point shape file containing SVF_v values at ground level, distributed throughout the city of Szeged.

Figure 5 shows the spatial distribution of the SVF_v values for selected areas representing different built-up types in Szeged. This figure illustrates the small-scale spatial variation of the SVF_v. The values are relatively low in the city centre, because of the narrow streets and small courtyards. In some parts of this area the values can reach about 0.1 and the highest values ($\sim$0.8)

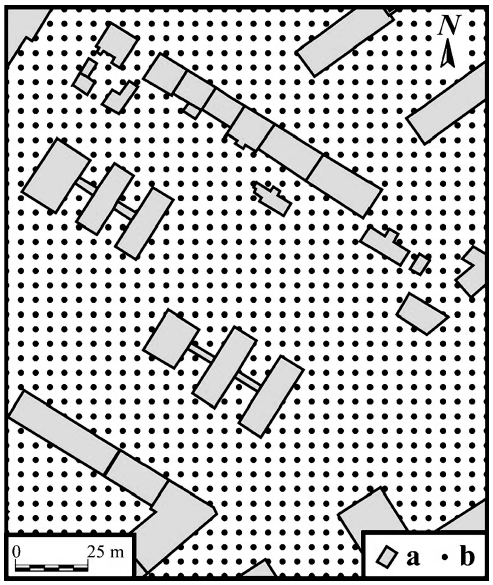

Fig. 4. A small part of the study area with (a) the building footprints and (b) the SVF measurement points at 5 m resolution for the vector based method

occur in parks (Fig. 5a). In the residential area, with mainly detached houses, the lowest SVF_v values are adjacent to the houses with minimum values of about 0.5 and there are open places where the SVF_v values are almost 1 (Fig. 5b). In the area with large apartment blocks the building density is relatively low but the SVF_v of about 0.6 covers a significant part of this cell. This is the effect of the sparse but high buildings (Fig. 5c). In industrial districts the buildings cover large areas but they are not very high, so SVF_v values lower than 1 are found only near the buildings (Fig. 5d).

3.2 SVF calculation using a raster DEM

Raster DEMs used in this type of studies can be relatively easy derived from a local governmental vector database (Lindberg 2007). Since municipality raw data is mainly used for planning purposes both spatial accuracy and precision is high which makes it possible to produce a detailed raster image. Some spatial information is always lost in the vector-raster conversion but the overall quality of the final DEM is satisfying (Fig. 6). The quality of the raster model depends on the chosen pixel size of the model and how de-

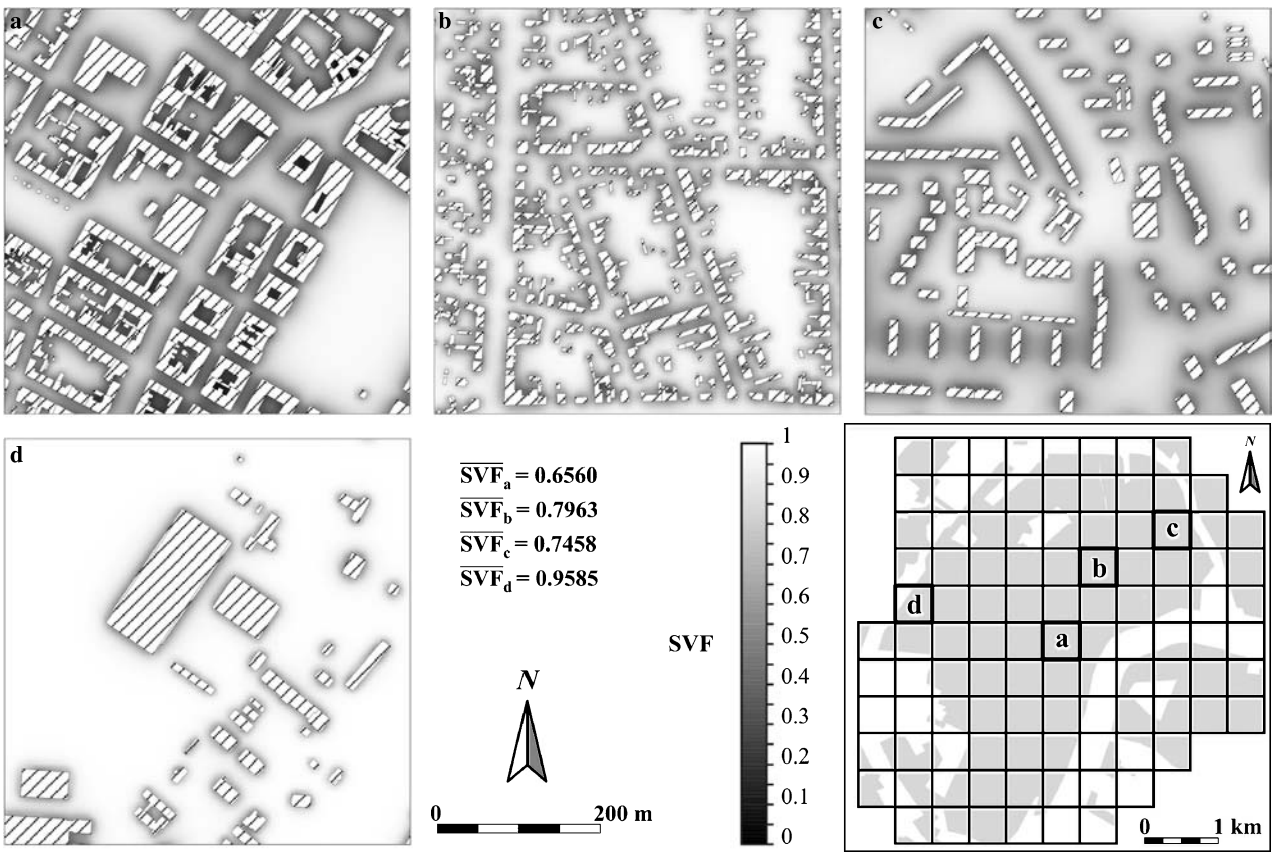

Fig. 5. Spatial distribution of SVF_v in some selected typical cells in Szeged and their averages

Fig. 6. The raster DEM converted from a 3D vector database covering the city of Szeged used in the current study (pixel resolution = 2 m)

tailed is the input vector-based information. Here we use a spatial resolution of 2 m for the raster DEM. Thus, a 1 m error is added in the vector-raster conversion. Clark Labs IDRISI Kilimanjaro© was used for the vector-raster conversion (www.clarklabs.org). By using a spatial resolution of 2 m, 7,562,500 pixels were used in the calculations.

A *shadow casting* algorithm developed by Ratti and Richens (1999) underlies our GIS-analysis. It is used to calculate shadow patterns on a raster image. The algorithm is fairly straightforward: the altitude and azimuth of a distant light source (the Sun) is used as input information together with the raster DEM (Fig. 7, left). Two basic image processing operations are included in the algorithm; (1) translation of the DEM in a given direction, and (2) reduction of building heights based on solar altitude. The approach taken is to compute 'shadow volumes' as a new DEM, that is, the upper surface of the atmospheric volume that is in shadow. First, three components of the vector pointing towards the Sun are defined based on solar altitude and azimuth. Then the opposite vector is used for further calculations. The largest of the x and y components

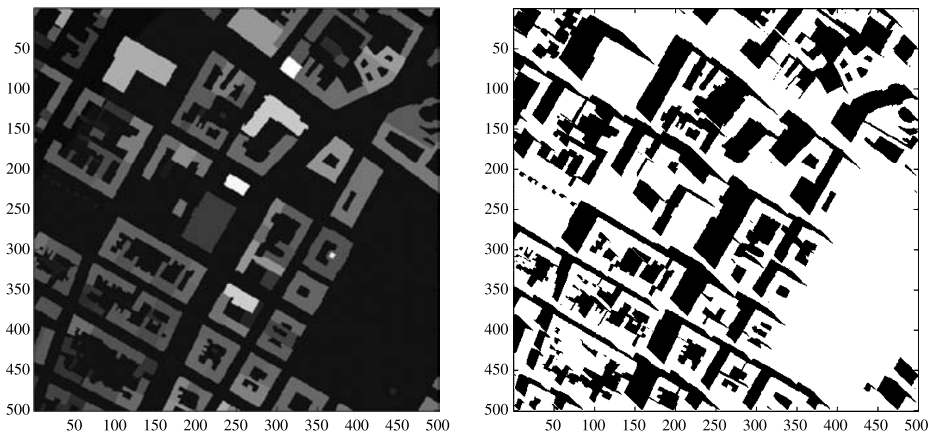

Fig. 7. *Left*: A section of the urban DEM of Szeged (pixel resolution 1 m). *Right*: Shadow patterns with a solar altitude of 25° and an azimuth angle of 135° (southeast)

are scaled so that the movement is equal to the pixel size of the DEM and the z component is used as a subtraction value for the translated DEM. If the DEM is translated by the x and y components and at the same time a reduction in height by the z component is made, part of the shadow volume is produced. By continuing translating and lowering by multiplies of the vector and taking the maximum of this volume with that previously calculated, the whole shadow volume is built up as a new DEM. The process is stopped when all levels are zero or translation has shifted the volume right off the image. To reduce the shadow volume to an actual map of shadows on the roofs and ground the original DEM is subtracted from the shadow volume and a Boolean image is produced where pixels with a negative or zero value are those exposed to sunlight and given a new value of 1, and positive values are in shade and given a new value of 0 (Fig. 7, right). For a more detailed description of the shadow casting algorithm, see Ratti (2001) and Ratti and Richens (2004).

By using the shadow casting algorithm it is possible to calculate SVF (given here as SVF_r – i.e. SVF computed by the raster based method) for all pixels in a DEM by generating 1000 shadow maps where solar altitude and azimuth are randomly chosen for each separate shadow map. To get correct SVF_r values, generated shadow images with computed vectors based on artificially large solar altitudes must have a higher weighted coefficient than a point closer to the horizon, according to heat transfer theory. This is done by using the sum of the cosine weighted elemental solid angles in the whole hemisphere. The SVF_r images are the average of the 1000 different shadow images produced. The shadow casting algorithm was validated by comparison between extracted values from a DEM and SVF values derived from hemispheric photographs in Göteborg with very satisfactory results (Lindberg 2005).

Investigating the spatial distribution of the SVF_r values for selected areas representing different built-up types in Szeged (Fig. 8), we get,

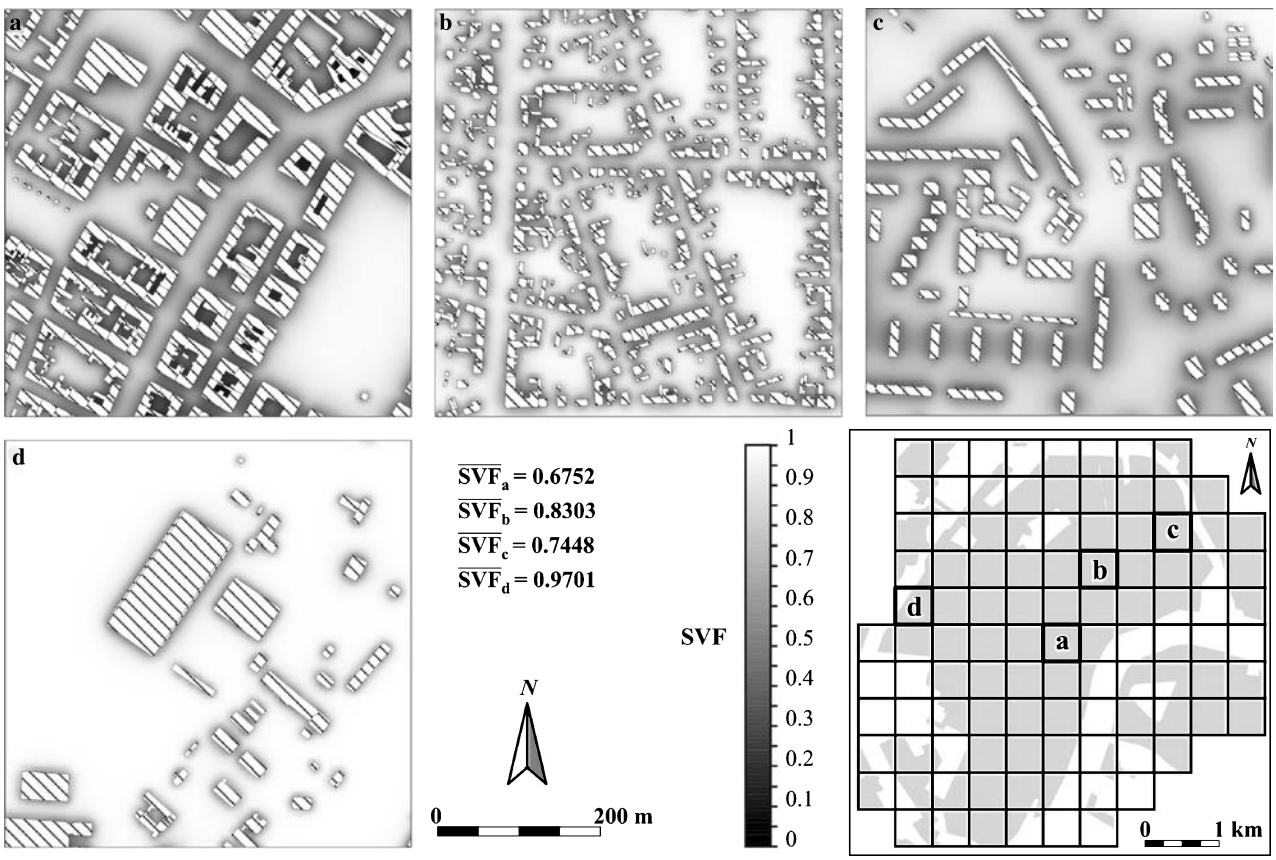

Fig. 8. Spatial distribution of SVF_r in some selected typical cells in Szeged and their averages

very similar pictures to the corresponding ones in Fig. 5.

4. Results of calculations

4.1 Spatial distributions of SVF values and comparison of methods

As a first step, we compare the calculated SVF values to the ones of the analytical method given by Oke (1987) for two idealized cases: (i) an infinitely-long canyon flanked by two parallel buildings of equal height (canyon width 20 m, building height 12 m) where the SVF calculation was done for the mid-point between the buildings, and (ii) a circular basin with walls of equal height (radius 10 m, wall height 12 m) where the SVF calculation was done for the centre point. The analytical computation used these equations (Oke 1987) is:

$$\mathrm{SVF}_{\mathrm{canyon}} = \cos^2\beta \quad \text{and} \quad \mathrm{SVF}_{\mathrm{basin}} = \cos\beta$$

where, β is the elevation angle from the centre to the wall.

As a second step, we calculated the SVF values with both of the methods for two idealized cases. The first is an infinitely-long canyon (in the calculation we used two 3 km long, 20 m wide and 12 m high buildings separated by a 20 m street). The second is a circular basin (in the calculation we used one circular 10 m high building with a 20 m wide space around the centre). Table 1 shows the vector method gives almost the same values as the analytical, while the raster method gives slightly larger values than the analytically computed value, but the difference is negligible.

Table 1. Result of comparison between $\mathrm{SVF_v}$, $\mathrm{SVF_r}$ and the SVF value using an analytic calculation for two idealized cases

	SVF in an infinitely-long canyon	SVF in a circular basin
$\mathrm{SVF_r}$	0.6543	0.4170
$\mathrm{SVF_v}$	0.6402	0.4086
$\mathrm{SVF_{analytic}}$	0.6402	0.4098

Figure 9 shows the spatial distribution of the cell averages of SVF calculated by the vector and raster based methods. The cell averages of $\mathrm{SVF_v}$ and $\mathrm{SVF_r}$ range between 0.616–0.999 and 0.641–0.999, respectively, in the study area of Szeged. It is generally true that cells located near the city border have high mean SVF values and cells near the centre have low values. However, among the sampled cells there are cells with low SVF values at the city border because of the large housing estates where high rise buildings are located (see also Fig. 5). In order to compare the cell averages of the two SVF methods, SVF differences were calculated for each cell: $\Delta_{\mathrm{SVF}} = \mathrm{SVF_v} - \mathrm{SVF_r}$ (Fig. 10). In most cases the differences are negative i.e. the $\mathrm{SVF_r}$ values are larger than $\mathrm{SVF_v}$. However, absolute values of the differences are less than 0.005 in one third of the study area. The largest deviation between the two methods is -0.037 and differences range from -0.025 to -0.037 in only 15% of the area. In cells where Δ_{SVF} differences are greater than -0.02 the built-up ratio is usually greater than 58% (Unger et al. 2001). From the city centre towards the suburbs the built-up ratio decreases as do Δ_{SVF} values.

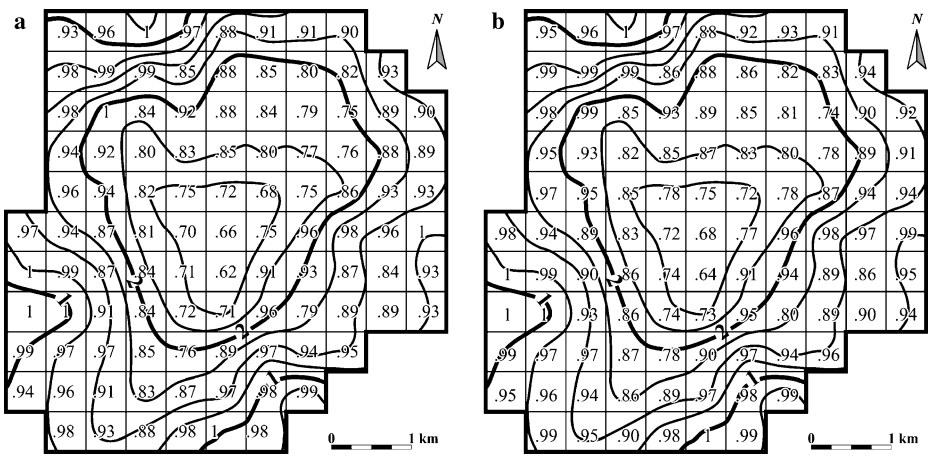

Fig. 9. Spatial distribution of (**a**) $\mathrm{SVF_v}$ (cell averages by vector based method) and (**b**) $\mathrm{SVF_r}$ (cell averages by raster based method), as well as the annual mean of ΔT [°C] (April 2002–March 2003) in Szeged

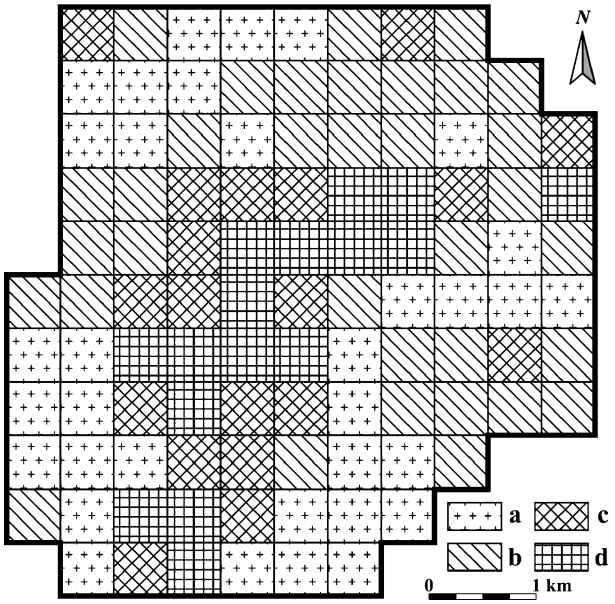

Fig. 10. Spatial distribution of the difference between the SVF values of cells calculated by the applied methods: $\Delta_{SVF} = SVF_v - SVF_r$ (a: $0.005 > \Delta_{SVF} \geq -0.005$; b: $-0.005 > \Delta_{SVF} \geq -0.015$; c: $-0.015 > \Delta_{SVF} \geq -0.025$; d: $-0.025 > \Delta_{SVF} \geq -0.037$)

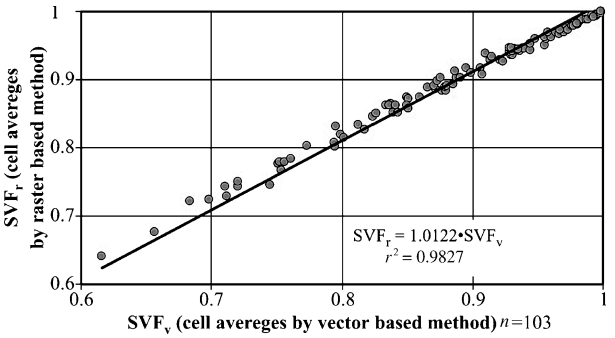

Fig. 11. Relationship between the cell averages of SVF calculated by the applied methods in Szeged ($n = 103$)

Figure 11 shows the regression line and the correlation between the cell averages by raster (SVF_r) and vector (SVF_v) based calculation. The deviation is minimal and the coefficient of determination (r^2) is 0.9827. The point of intersection of the regression line with the y axis is at the origin. The slope coefficient of SVF_v is a bit larger than 1 ($\sim$1.012) which confirms that differences between the two methods are small and mostly negative, i.e. SVF_r values are slightly larger than the corresponding SVF_v values.

This slight difference can be explained in the following way. As we earlier mentioned, there is some tendency in the difference between the raster and vector based methods depending on the location of the cells within the urban area. In the central (densely built-up) areas the average SVF_r values are higher than the corresponding SVF_v values. The possible reason for this lies in differences between the raster and vector based calculations (Fig. 12). In most cases the smallest SVF values can be found near the walls of buildings. Applying the vector based method we include this small individual SVF_v value in the calculation of the cell average. On the other hand, with the raster based method the SVF_r value at a point which is closer to the wall than half the pixel resolution cannot be calculated because the centre of the pixel overlaps the building (the SVF_r value should refer to the roof) so it is not included in the pixels used to calculate the cell average. In areas where the built-up ratio is high this situation is frequently encountered so differences between the two SVF cell averages are larger.

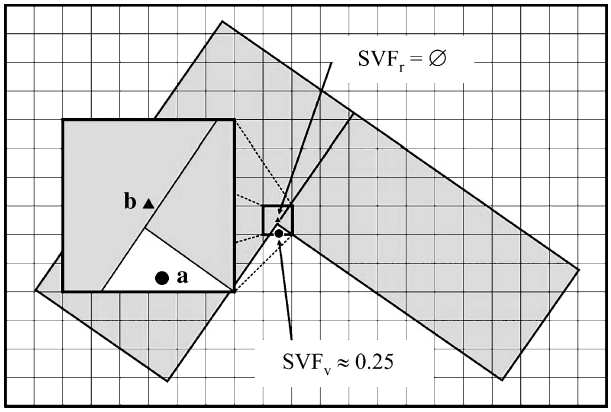

Fig. 12. The different approaches of the raster and vector based method (a: SVF measurement point, b: centre of the pixel)

There are two other factors causing cell averages of SVF_r to be slightly higher than cell averages of SVF_v at high values of average SVF. Firstly, ground elevation is included in the raster DEM which could increase SVF_r in certain areas to a small extent. Secondly, the vector method only includes buildings within a distance of less than 200 m from the point of SVF calculation. If buildings outside that proximity were included, increased hemispheric obstruction would have resulted in smaller SVF_v. The shadow casting algorithm used in the raster method has no such horizontal limitation except for the boundaries of the DEM itself. The reason why the difference between SVF_r and SVF_v is higher

in the cells with high built-up areas is because the mean height of the buildings is usually higher in those cells.

4.2 Limitations, possibilities

Local municipality data can be very suitable in the production of a high resolution DEM of urban geometry. One limitation is that the conversion from vector to raster format results in loss of information, another limitation is data accessibility. Datasets that include building heights are still rare.

The advantage of using raster images instead of vector data is the possibility to examine larger areas (e.g. cities) because geometric calculations are faster. The computation time of the shadow casting algorithm increases quadratically as the number of pixels increases. Hence, if large areas are to be studied image resolution must be decreased to speed up the computation. The computation time of the SVF_r image covering Szeged ($n = 7{,}562{,}500$) was 38 h of a regular PC whereas it takes 12 days with the vector based method. Lindberg (2005) shows that in the city centre of Göteborg (mean canyon width = 7 m) pixel size can be increased to approximately half the canyon width i.e. 4 metres without any appreciable loss of information and therefore computational time is decreased.

5. Application – UHI-SVF relationship in Szeged

First, we examine the spatial distribution of annual mean ΔT calculated from the 35 nights of measurement (see Sect. 2). The effects of different weather conditions (more or less favourable for heat island development) are amalgamated in these ΔT averages. Figure 9 shows the most obvious feature of the yearly UHI pattern is the almost concentric shape of the isotherms. Highest ΔT values are found in the centre (>2.5 °C) and the mean ΔT ranges between 0.74 and 2.72 °C within the study area. A deviation from this shape occurs in the north-eastern part of the city, where the isotherms stretch towards the suburbs. This can be explained by the effect of the large housing estates with high concrete buildings that are mainly located there. A second irregularity may be due to the cooling influence of river Tisza. Along the river isotherms are drawn back a bit towards the centre (see also Fig. 1). The third irregularity can be found in the western part of the city, where large open (green) areas are located (see also Fig. 1).

Secondly, we examine the relationship between the intra-urban variations of SVF and ΔT. Low SVF values occur together with high UHI intensities in the central parts and *vice versa* in the suburbs (Fig. 9). The ''toes'' of the isotherms (e.g. in the north-eastern part of the area) are in line with the drop of the SVF. Since there are no significant differences in the magnitudes and in the intra-urban variations of SVF_v and SVF_r (Fig. 9a and b) these interpretations apply to sets.

In order to demonstrate the above mentioned relationship, linear regression is used, where the applied parameters (as cell averages) are the following:

(i) independent variable: sky view factor (SVF_v or SVF_r),
(ii) dependent variable: annual mean UHI intensity (ΔT_{year}).

There is a strong linear connection between SVF_v and ΔT_{year} in the studied urban area (Fig. 13). According to the statistical measures, about 63% of the intra-urban variations of temperature excess can be explained by variations of SVF. The relation is inverse (i.e. negative) at the 1% level of significance ($n = 103$). Applying SVF_r as the independent variable gives very similar results (Table 2). This is about a 15–20%) improvement in explanation compared to earlier work in Szeged (Table 2). In the first of the earlier studies the SVF was determined by an

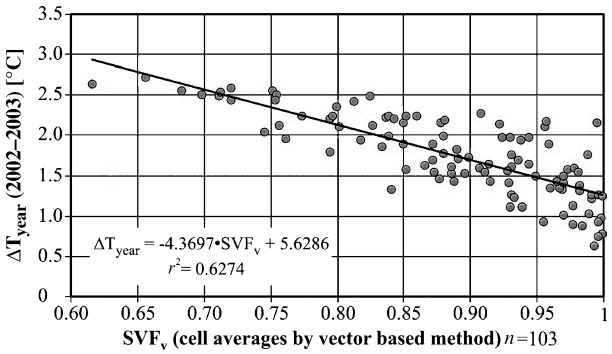

Fig. 13. Relationship between the SVF_v and ΔT_{year} in Szeged ($n = 103$)

Table 2. Relationship between the annual mean heat island (ΔT_{year}) and the sky view factor calculated by different methods and for different point sets ($SVF_{v(route)}$, $SVF_{v(route)}$, SVF_v, SVF_r)

Method of SVF calculation	Regression equation	r	r^2	Significance level (%)	Source
Analytic	$\Delta T_{year} = -4.62 \times SVF_{s(route)} + 5.90$	−0.689	0.4746	1	Unger (2004)
Vector based	$\Delta T_{year} = -4.06 \times SVF_{v(route)} + 5.50$	−0.653	0.4265	1	Unger (2007)
	$\Delta T_{year} = -4.37 \times SVF_v + 5.63$	−0.790	0.6274	1	Current study
Raster based	$\Delta T_{year} = -4.76 \times SVF + 6.03$	−0.795	0.6320	1	Current study

analytical (surveying) method (referred to as $SVF_{s(route)}$) in which two elevation angles to the top of the buildings were measured normal to the axis of streets in both directions at points along the measurement route at 125 m intervals in the same study area (Bottyán and Unger 2003; Unger 2004). In the second study the SVF was determined by the vector based method (referred to as $SVF_{v(route)}$) used in the present study, but the calculations were applied at points along the same route in 20 m intervals (Unger 2007).

6. Conclusions

Two different methods to derive continuous images of SVF covering large urban areas are examined. The first method utilizes a vector based algorithm whereas the second one computes SVF using a high resolution raster DEM. The spatial data consists of 3D building structures and ground elevation. Relationship between urban geometry, quantified by SVF, and variations of intra-urban nocturnal air temperature are also investigated. Results show that:

(i) Both methods result in very similar values for urban geometry.

(ii) By using the vector based method small SVF_v values (e.g. at the points closer to walls than half the pixel resolution) can be included in the calculation of the cell average. When averaging SVF over a large area (e.g. 500 by 500 m) an insignificant overestimation occurs using the raster based method.

(iii) The raster based method is significantly faster than the vector based method.

The study utilized a large number of areal means of SVF and ΔT. Values were related to a large sample area and based on numerous measurements. Measured temperature values at sites might show large variations because of the influence of microvariations of the immediate environments. Moreover, these values can be affected by advective effects from a wider environment (source area). Therefore, the applied areas extended over several blocks in the city.

(iv) In clarifying the SVF-UHI relationship the usefulness of the suggestion by Unger (2004, 2007) of applying areal means is confirmed. In accord with previous work the results in Szeged confirm that urban surface geometry (described by SVF) is a significant determining factor of the air temperature distribution inside the city. Both the vector and the raster approaches of deriving areal means of SVF are shown to be powerful ways to obtain a general picture of the geometric conditions for relatively large urban environments.

Acknowledgements

This research was supported by the Hungarian Scientific Research Fund (OTKA T/049573) and by FORMAS, the Swedish Research Council for Environment, Agricultural Sciences and Spatial Planning. Helpful comments from anonymous reviewers are acknowledged. Special thanks to Tim Oke for his additional comments and clarifying editorial work on the manuscript.

References

Bottyán Z, Unger J (2003) A multiple linear statistical model for estimating the mean maximum urban heat island. Theor Appl Climatol 75: 233–243

Brown MJ, Grimmond CSB, Ratti C (2001) Comparison of methodologies for computing sky view factor in urban environment. International Society of Environmental Hydraulics Conference, Tempe, AZ. Internal Report Los Alamos National Laboratory, Los Alamos, NM, LA-UR-01-4107

Eliasson I (1996) Urban nocturnal temperatures, street geometry and land use. Atmos Environ 30: 379–392

Goh KC, Chang CH (1999) The relationship between height to width ratios and the heat island intensity at 22:00 h for Singapore. Int J Climatol 19: 1011–1023

Grimmond CSB, Oke TR (1999) Aerodynamic properties of urban areas derived from analysis of surface form. J Appl Meteorol 38: 1262–1292

Landsberg HE (1981) The urban climate. Academic Press, New York

Lindberg F (2005) Towards the use of local governmental 3-D data within urban climatology studies. Mapping Image Sci 2: 32–37

Lindberg F (2007) Modelling the urban climate using a local governmental geo-database. Meteorol Appl 14: 263–273

Oke TR (1981) Canyon geometry and the nocturnal urban heat island: comparison of scale model and field observations. J Climatol 1: 237–254

Oke TR (1982) The energetic basis of the urban heat island. Quart J Roy Meteor Soc 108: 1–24

Oke TR (1987) Boundary layer climates. Routledge, London, New York

Oke TR (1988) Street design and urban canopy layer climate. Energ Buildings 11: 103–113

Oke TR (2004) Initial guidance to obtain representative meteorological observation sites. Instruments and Methods of Observation Programme, IOM Report No. 81, WMO/TD No. 1250, Geneva, 51 pp

Ratti CF (2001) Urban analysis for environmental prediction. Darwin College, University of Cambridge, 331 pp

Ratti CF, Richens P (1999) Urban texture analysis with image processing techniques. Proceed CAADFutures99, Atlanta, GA

Ratti CF, Richens P (2004) Raster analysis of urban form. Environ Plann B: Planning Design 31: 297–309

Souza LCL, Rodrigues DS, Mendes JFG (2003) The 3DSkyView extension: an urban geometry acces tool in a geographical information system. In: Klysik K, Oke TR, Fortuniak K, Grimmond CSB, Wibig J (eds) Proc. Fifth Int. Conf. on Urban Climate, Vol. 2. University of Lodz, Lodz, Poland, pp 413–416

Streutker DR (2003) Satellite-measured growth of the urban heat island of Houston, Texas. Remote Sens Environ 85: 282–289

Svensson M (2004) Sky view factor analysis – implications for urban air temperature differences. Meteorol Appl 11: 201–211

Unger J (1996) Heat island intensity with different meteorological conditions in a medium-sized town: Szeged, Hungary. Theor Appl Climatol 54: 147–151

Unger J (2004) Intra-urban relationship between surface geometry and urban heat island: review and new approach. Climate Res 27: 253–264

Unger J (2006) Modelling of the annual mean maximum urban heat island with the application of 2 and 3D surface parameters. Climate Res 30: 215–226

Unger J (2007) Connection between urban heat island and sky view factor approximated by a software tool on a 3D urban database. Int J Environ Pollut (in press)

Unger J, Sümeghy Z, Gulyás Á, Bottyán Z, Mucsi L (2001) Land-use and meteorological aspects of the urban heat island. Meteorol Appl 8: 189–194

Watson ID, Johnson GT (1987) Graphical estimation of sky view-factors in urban environments. J Climatol 7: 193–197

www.esri.com (2006)

www.clarklabs.org (2006)